Non-Parametric Shape Optimization of 3-D Frame Structures for Maximizing a Natural Frequency

***Takashi Morimoto[1] and Masatoshi Shimoda[2]**

[1] Department of Advanced Science and Technology, Graduate School of Engineering, Toyota Technological Institute,
[2]Department of Advanced Science and Technology, Toyota Technological Institute,
2-12-1 Hisakata, Tenpaku-ku, Nagoya, 468-8511, Japan

*Corresponding author: sd12443@toyota-ti.ac.jp

Abstract

This paper presents a non-parametric, or a node-based, shape optimization method for designing the optimal geometry of a 3-D frame structure composed of arbitrarily curved linear elastic members. A design problem dealt with maximizing the natural frequency of a specified mode is formulated as a distributed-parameter shape optimization problem. Under the assumption of that each member varies in the normal direction to its centroidal axis, the shape gradient function and the optimality conditions are theoretically derived by the Lagrange multiplier method and the material derivative method. The optimal free-form geometry is determined by applying the derived shape gradient function as the fictious external forces to the members to minimize the objective functional, which is referred as the free-form optimization method for frame structures, a gradient method in a Hilbert space, proposed by the authors. The effectiveness and validity of the proposed method is verified through several design problems.

Keywords: Shape Optimization, Parameter-Free, Free-Form, Frame Structure, Space Frame

Introduction

Structures composed of thin straight or curved members are classified as frame structures, which are widely utilized in the fields of engineering. Large stadiums, bridges, and radio towers are the typical examples in urban architecture and civil engineering. The lightness and slenderness are the favorable features as they are resource saving and eco-friendly; however, these features are apt to result in a lack of stiffness, which may be a cause of noise or vibration. To avoid undesirable vibration modes to be dominant and incur noise or fatigue of the composing members when a frame structure is exited, it is important to optimize the natural frequency, or the eigenvalue, for designing a frame structure. In the early stages of the design process, the shape can often be treated as the design variables, and in that case, the mechanical characteristics can be dramatically improved rather than optimizing the cross sectional shapes or sizes. Up to today, various numerical shape optimization methods for frame structures have been proposed. For instance, Wang, *et al*. (2004) reported simultaneous shape and sizing optimization to minimize the weight under multiple frequency constraints by calculating the integrated discrete sensitivity numbers. Ohsaki and Fujita (2011) applied the SQP method to multi-objective shape optimization of latticed shells parameterized by a Bezier surface. Numbers of heuristic approaches have also been reported; Hashemian *et al.* (2011) applied the genetic algorithm (GA) method for a squared lattice cylindrical shell under a compressive axial load to achieve a maximum buckling load. Kaveh and Bakhshpoori (2013) reported optimum design of space trusses for achieving minimum weight subjected to the stress limitations using the Cuckoo search algorithm (CS) with Levy flights. These are categorized in the parametric methods; however, few non-parametric methods have been reported, and considering the possible number of members and degrees of freedom of a frame structure, a shape

optimization method that can efficiently solve a large scale problem has much utility value. The authors proposed the free-form optimization method for frame structures taking up the stiffness maximization problems (Shimoda, *et al.* ,2013). It is a node-based, gradient method in a Hilbert space, and it can treat all nodes as design variables and provide a smoothly curved optimal free-form shape. In this study, we applied this method to natural vibration problems that aim to maximize a specified vibration eigenvalue while tracking its natural vibration mode. In the following sections, we will describe a non-parametric shape optimization problem for frame structures, a formulation of the problem and the shape gradient function, the free-form optimization method for frame structures, and calculated design examples.

Non-parametric shape optimization problem of frame structures

Governing equation of frame structure

As shown in Fig.1, a frame structure is defined as an assembly of arbitrarily curved members $\{\Omega^j\}_{j=,2,\ldots,N}$, and each member is consisted of piecewise straight Timoshenko beams, which is used for applicability to a wide range of problems by considering shear deformation. The frame structure occupies a bounded domain ($\Omega \subset \mathbb{R}^3, \Omega = \bigcup_{j=1}^{N} \Omega^j$), N representing the number of members. The notation (x_1^j, x_2^j, x_3^j) and (X_1, X_2, X_3) indicates the local coordinate system with respect to the j th member and the global coordinate system, respectively,

$$\Omega^j = \left\{ \left(x_1^j, x_2^j, x_3^j \right) \in \mathbb{R}^3 \middle| \left(x_1^j, x_2^j \right) \in A^j \subset \mathbb{R}^2,\ x_3^j \in S^j \subset \mathbb{R} \right\},\ \Gamma^j = \partial A^j \times S^j,\ \Omega^j = A^j \times S^j, \tag{1}$$

where S^j, A^j and Γ^j express the j th member's centroidal axis, cross section, and circumference surface except the end faces, respectively. Note that, for the sake of avoiding complex notations, the superscript j will often be omitted in the following sections unless necessary. The weak form of the governing equation of natural vibration is expressed as Eq. (2), where $\boldsymbol{w} = \{w_i\}_{i=1,2,3}$ denotes the transverse displacement vector in x_1, x_2, x_3 direction, and $\boldsymbol{\theta} = \{\theta_i\}_{i=1,2,3}$ denotes the rotation vector related to the x_1, x_2, x_3 axis.

$$a\left(\left(\boldsymbol{w}^{(r)}, \boldsymbol{\theta}^{(r)} \right), \left(\bar{\boldsymbol{w}}, \bar{\boldsymbol{\theta}} \right) \right) = \lambda^{(r)} b\left(\left(\boldsymbol{w}^{(r)}, \boldsymbol{\theta}^{(r)} \right), \left(\bar{\boldsymbol{w}}, \bar{\boldsymbol{\theta}} \right) \right),\ \forall \left(\bar{\boldsymbol{w}}, \bar{\boldsymbol{\theta}} \right) \in U,\ (\boldsymbol{w}, \boldsymbol{\theta}) \in U, \tag{2}$$

where $(\cdot)^{(r)}$ denotes the eigenvector of r th natural mode and $\lambda^{(r)}$ denotes its eigenvalue. Moreover, the notation $\bar{(\cdot)}$ expresses a variation, and U expresses the admissible function space in which the given constraint conditions of $(\boldsymbol{w}, \boldsymbol{\theta})$ are satisfied. The bilinear form $a(\cdot,\cdot)$ and $b(\cdot,\cdot)$ are defined respectively, as shown below:

$$\begin{aligned} a\left(\left(\boldsymbol{w}^{(r)}, \boldsymbol{\theta}^{(r)} \right), \left(\bar{\boldsymbol{w}}, \bar{\boldsymbol{\theta}} \right) \right) = & \sum_{j=1}^{N} \int_{\Omega^j} \left\{ \left(w_{1,3}^{(r)} - x_2 \theta_{3,3}^{(r)} - \theta_2^{(r)} \right) \mu \left(\bar{w}_{1,3} - x_2 \bar{\theta}_{3,3} - \bar{\theta}_2 \right) \right. \\ & + \left(w_{2,3}^{(r)} + x_1 \theta_{3,3}^{(r)} + \theta_1^{(r)} \right) \mu \left(\bar{w}_{2,3} + x_1 \bar{\theta}_{3,3} + \bar{\theta}_1 \right) \\ & \left. + \left(w_{3,3}^{(r)} - x_1 \theta_{2,3}^{(r)} + x_2 \theta_{1,3}^{(r)} \right) E \left(\bar{w}_{3,3} - x_1 \bar{\theta}_{2,3} + x_2 \bar{\theta}_{1,3} \right) d\Omega, \end{aligned} \tag{3}$$

$$\begin{aligned} b\left(\left(\boldsymbol{w}^{(r)}, \boldsymbol{\theta}^{(r)} \right), \left(\bar{\boldsymbol{w}}, \bar{\boldsymbol{\theta}} \right) \right) = & \sum_{j=1}^{N} \int_{\Omega^j} \rho \left\{ \left(w_1^{(r)} - x_2 \theta_3^{(r)} \right) \left(\bar{w}_1 - x_2 \bar{\theta}_3 \right) + \left(w_2^{(r)} + x_1 \theta_3^{(r)} \right) \left(\bar{w}_2 + x_1 \bar{\theta}_3 \right) \right. \\ & \left. + \left(w_3^{(r)} - x_1 \theta_2^{(r)} + x_2 \theta_1^{(r)} \right) \left(\bar{w}_3 - x_1 \bar{\theta}_2 + x_2 \bar{\theta}_1 \right) \right\} d\Omega, \end{aligned} \tag{4}$$

where μ, E, ρ denote the Lamé parameters, the Young's modulus, and the material density, respectively. Moreover, the tensor subscript notation uses Einstein's summation convention and a partial differential notation for the spatial coordinates $(\cdot)_{,i} = \partial(\cdot)/\partial x_i$.

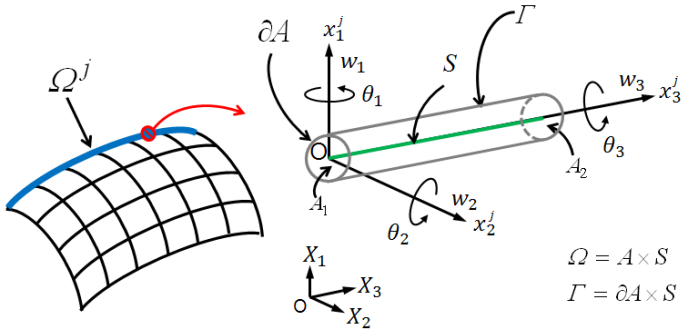

Figure 1. Frame structure composed of members consisting of Timoshenko beams

Domain variation

In the frame structure shown in Fig. 2, we consider that member *j* having an initial domain Ω^j and the centroidal axis S^j undergoes the domain variation $\boldsymbol{V}^j$ (design velocity field) in the normal direction to the axis such that its domain and axis become Ω_s^j and S_s^j, respectively. The subscript *s* expresses the iteration histories of the domain variation. Defining the notation $\boldsymbol{n}_1$ and $\boldsymbol{n}_2$ as outward unit normal vectors of the centroidal axis in the $\boldsymbol{x}_1$ and $\boldsymbol{x}_2$ directions, $\boldsymbol{V}^j$ can be expressed by:

$$\boldsymbol{V}^j = \left(\boldsymbol{V}^j \cdot \boldsymbol{n}_1^j\right)\boldsymbol{n}_1^j + \left(\boldsymbol{V}^j \cdot \boldsymbol{n}_2^j\right)\boldsymbol{n}_2^j. \tag{5}$$

In this study, a beam of a uniform rectangular cross section with height h_1 and width h_2 is considered as shown in Fig. 3. The relationships of $\left(\boldsymbol{V}\cdot\boldsymbol{n}^t\right)\boldsymbol{n}^t = \left(-\boldsymbol{V}\cdot\boldsymbol{n}^b\right)\boldsymbol{n}^b$ and $\left(\boldsymbol{V}\cdot\boldsymbol{n}^r\right)\boldsymbol{n}^r = \left(-\boldsymbol{V}\cdot\boldsymbol{n}^l\right)\boldsymbol{n}^l$ are assumed by using the notations $\boldsymbol{n}^t$, $\boldsymbol{n}^b$, $\boldsymbol{n}^r$ and $\boldsymbol{n}^l$, which denote the unit outward normal vector at the top, bottom, right and left edges of the cross section, respectively. Moreover, $\boldsymbol{n}_1$, $\boldsymbol{n}_2$ denote unit vectors of the centroid in the directions of axis $\boldsymbol{x}_1$ and $\boldsymbol{x}_2$, and then they have the relationships of $\boldsymbol{n}_1 = \boldsymbol{n}^t = -\boldsymbol{n}^b$, $\boldsymbol{n}_2 = \boldsymbol{n}^r = -\boldsymbol{n}^l$, respectively.

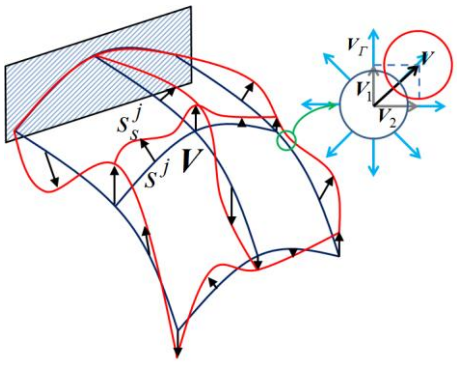

Figure 2. Shape variation

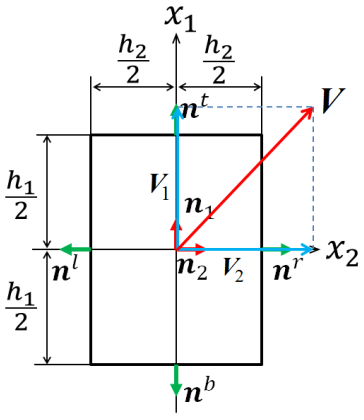

Figure 3. Sign notation of cross section

Eigenvalue maximization problem and the shape gradient function

With the aim of maximizing the specified order r th vibration eigenvalue $\lambda^{(r)}$, or minimizing -$\lambda^{(r)}$, introducing the natural vibration equation stated in Eq.(2) and the maximum allowable volume as the constraint conditions, the shape optimization problems for finding $\boldsymbol{V}$ can be formulated as:

$$\textit{Given} \quad \Omega, \tag{6}$$

$$\textit{find} \quad \boldsymbol{V} \text{ or } \Omega_s, \tag{7}$$

$$\textit{that minimizes} \quad -\lambda^{(r)}, \tag{8}$$

$$\textit{subject to} \quad \text{Eq. (2) } \textit{and} \quad M\left(=\sum_{j=1}^{N}\int_{S^j} A dS\right) \le \hat{M}, \tag{9}$$

where M and $\hat{M}$ denote the volume and its constraint value, respectively.
As the order of the specified mode may differ from the one at the initial shape after the shape is updated, MAC (Modal Assurance Criterion) is introduced for tracking the specified mode. MAC value is calculated by the following equation,

$$MAC(\boldsymbol{\phi}_0^{(r)}, \boldsymbol{\phi}_s^{(i)}) = \frac{\left|\boldsymbol{\phi}_0^{(r)T}\boldsymbol{\phi}_s^{(i)}\right|^2}{\left(\boldsymbol{\phi}_0^{(r)T}\boldsymbol{\phi}_0^{(r)}\right)\left(\boldsymbol{\phi}_s^{(i)T}\boldsymbol{\phi}_s^{(i)}\right)}. \tag{10}$$

The notation $\boldsymbol{\phi}_0^{(r)}$ denotes the specified r th eigenvector of the initial shape. $\boldsymbol{\phi}_s^{(i)}$ denotes the i th eigenvector (i =1 to the maximum analysis order) of the shape after s number of times updated, and the superscript T denotes the transpose of a vector. The mode that has the maximum MAC value in all modes is regarded as the corresponding mode to be tracked.
Allowing $(\bar{\boldsymbol{w}}, \bar{\boldsymbol{\theta}})$ and Λ denote the Lagrange multipliers for the specified natural vibration equation and the volume constraint, respectively, the Lagrange functional L associated with this problem can be expressed as

$$L\left(\Omega, \left(\boldsymbol{w}^{(r)}, \boldsymbol{\theta}^{(r)}\right), \left(\bar{\boldsymbol{w}}, \bar{\boldsymbol{\theta}}\right), \Lambda\right) = -\lambda^{(r)} + \lambda^{(r)} b\left(\left(\boldsymbol{w}^{(r)}, \boldsymbol{\theta}^{(r)}\right), \left(\bar{\boldsymbol{w}}, \bar{\boldsymbol{\theta}}\right)\right) - a\left(\left(\boldsymbol{w}^{(r)}, \boldsymbol{\theta}^{(r)}\right), \left(\bar{\boldsymbol{w}}, \bar{\boldsymbol{\theta}}\right)\right) + \Lambda\left(M - \hat{M}\right). \tag{11}$$

The material derivative $\dot{L}$ of the Lagrange functional can be derived as shown in Eq. (12) using the design velocity field of the centroidal axis $\boldsymbol{V}$, the design velocity field on the circumference surface $\boldsymbol{V}_{\Gamma}$, and an outward unit normal vector $\boldsymbol{n}$ on the centroidal axis or the virtual cross section.

$$\begin{aligned}\dot{L} = {} & \dot{\lambda}^{(r)}\left\{b\left(\left(\boldsymbol{w}^{(r)}, \boldsymbol{\theta}^{(r)}\right), \left(\bar{\boldsymbol{w}}, \bar{\boldsymbol{\theta}}\right)\right) - 1\right\} + \lambda^{(r)} b\left(\left(\boldsymbol{w}^{(r)\prime}, \boldsymbol{\theta}^{(r)\prime}\right), \left(\bar{\boldsymbol{w}}, \bar{\boldsymbol{\theta}}\right)\right) + \lambda^{(r)} b\left(\left(\boldsymbol{w}^{(r)}, \boldsymbol{\theta}^{(r)}\right), \left(\bar{\boldsymbol{w}}', \bar{\boldsymbol{\theta}}'\right)\right) \\ & - a((\boldsymbol{w}^{(r)\prime}, \boldsymbol{\theta}^{(r)\prime}), (\bar{\boldsymbol{w}}, \bar{\boldsymbol{\theta}})) - a((\boldsymbol{w}^{(r)}, \boldsymbol{\theta}^{(r)}), (\bar{\boldsymbol{w}}', \bar{\boldsymbol{\theta}}')) + \dot{\Lambda}\left(M - \hat{M}\right) + \left\langle G\boldsymbol{n}, \boldsymbol{V}\right\rangle, \ \boldsymbol{V} \in \mathrm{C}_{\Theta}\end{aligned} \tag{12}$$

$$\begin{aligned}\left\langle G\boldsymbol{n}, \boldsymbol{V}\right\rangle &\equiv \sum_{j=1}^{N}\left\{\int_{\Gamma^j} G\boldsymbol{V}_{\Gamma}\cdot\boldsymbol{n}\, d\Gamma + \int_{S^j} G_0\boldsymbol{V}\cdot\boldsymbol{n}\, dS\right\} \\ &= \sum_{j=1}^{N}\left[-\int_{\Gamma^j}\left\{\left(w_{1,3}^{(r)} - x_2\theta_{3,3}^{(r)} - \theta_2^{(r)}\right)\mu\left(\bar{w}_{1,3} - x_2\bar{\theta}_{3,3} - \bar{\theta}_2\right) + \left(w_{2,3}^{(r)} - x_1\theta_{3,3}^{(r)} + \theta_1^{(r)}\right)\mu\left(\bar{w}_{2,3} + x_1\bar{\theta}_{3,3} + \bar{\theta}_1\right)\right.\right.\end{aligned}$$

$$+\left(w_{3,3}^{(r)}-x_1\theta_{2,3}^{(r)}+x_2\theta_{1,3}^{(r)}\right)E\left(\bar{w}_{3,3}-x_1\bar{\theta}_{2,3}+x_2\bar{\theta}_{1,3}\right)\Big\}\boldsymbol{V}_\Gamma\cdot\boldsymbol{n}\,d\Gamma$$
$$+\int_{\Gamma^j}\lambda^{(r)}\rho\Big\{\left(w_1^{(r)}-x_2\theta_3^{(r)}\right)\left(\bar{w}_1-x_2\bar{\theta}_3\right)+\left(w_2^{(r)}+x_1\theta_3^{(r)}\right)\left(\bar{w}_2+x_1\bar{\theta}_3\right)$$
$$+\left(w_3^{(r)}-x_1\theta_2^{(r)}+x_2\theta_1^{(r)}\right)\left(\bar{w}_3-x_1\bar{\theta}_2+x_2\bar{\theta}_1\right)\Big\}\boldsymbol{V}_\Gamma\cdot\boldsymbol{n}\,d\Gamma$$
$$+\int_{S^j}\Lambda AH\boldsymbol{V}\cdot\boldsymbol{n}dS\Big], \tag{13}$$

where $G\boldsymbol{n}$ ($\equiv\boldsymbol{G}$) expresses the shape gradient function (i.e., sensitivity function), which is a coefficient function in terms of $\boldsymbol{V}_\Gamma$ or $\boldsymbol{V}$, and the notation H denotes the curvature of the centroidal axis. The notations $(\cdot)'$ and $\dot{(\cdot)}$ are the shape derivative and the material derivative with respect to the domain variation, respectively (Choi and Kim, 2005).
The optimality conditions of the Lagrange functional L with respect to $(\boldsymbol{w}^{(r)},\boldsymbol{\theta}^{(r)})$, $(\bar{\boldsymbol{w}},\bar{\boldsymbol{\theta}})$ and Λ are expressed as:

$$a\left(\left(\boldsymbol{w}^{(r)},\boldsymbol{\theta}^{(r)}\right),\left(\bar{\boldsymbol{w}}',\bar{\boldsymbol{\theta}}'\right)\right)=\lambda^{(r)}b\left(\left(\boldsymbol{w}^{(r)},\boldsymbol{\theta}^{(r)}\right),\left(\bar{\boldsymbol{w}}',\bar{\boldsymbol{\theta}}'\right)\right),\ \ \forall\left(\bar{\boldsymbol{w}}',\bar{\boldsymbol{\theta}}'\right)\in U, \tag{14}$$
$$a\left(\left(\boldsymbol{w}^{(r)\prime},\boldsymbol{\theta}^{(r)\prime}\right),\left(\bar{\boldsymbol{w}},\bar{\boldsymbol{\theta}}\right)\right)=\lambda^{(r)}b\left(\left(\boldsymbol{w}^{(r)\prime},\boldsymbol{\theta}^{(r)\prime}\right),\left(\bar{\boldsymbol{w}},\bar{\boldsymbol{\theta}}\right)\right),\ \ \forall\left(\boldsymbol{w}^{(r)\prime},\boldsymbol{\theta}^{(r)\prime}\right)\in U, \tag{15}$$
$$b\left(\left(\boldsymbol{w}^{(r)},\boldsymbol{\theta}^{(r)}\right),\left(\bar{\boldsymbol{w}},\bar{\boldsymbol{\theta}}\right)\right)=1, \tag{16}$$
$$\dot{\Lambda}\left(M-\hat{M}\right)=0,\ M-\hat{M}\le 0,\ \Lambda\ge 0. \tag{17)(18)(19}$$

When the optimality conditions are satisfied, $\dot{L}$ becomes:

$$\dot{L}=\left\langle G\boldsymbol{n},\boldsymbol{V}\right\rangle. \tag{20}$$

Considering the self-adjoint relationship, $\left(\boldsymbol{w}^{(r)},\boldsymbol{\theta}^{(r)}\right)=\left(\bar{\boldsymbol{w}},\bar{\boldsymbol{\theta}}\right)$ obtained by Eq.(14) and Eq.(15) and $\int_{\Gamma^j}(\cdot)d\Gamma=\int_{S^j}\int_{\partial A}(\cdot)dAdS$, the shape gradient density functions, G_1,G_2,G_0, are derived in the following equations.

$$\left\langle Gn,V\right\rangle=\sum_{j=1}^{N}\int_{S^j}\left\{G_1\boldsymbol{V}\cdot\boldsymbol{n}_1+G_2\boldsymbol{V}\cdot\boldsymbol{n}_2+G_0\boldsymbol{V}\cdot\boldsymbol{n}_1\right\}dS, \tag{21}$$
$$G_1=2h_1h_2\left\{Ew_{3,3}^{(r)}\theta_{2,3}^{(r)}-\mu\theta_{3,3}^{(r)}\left(w_{2,3}^{(r)}+\theta_1^{(r)}\right)+\lambda^{(r)}\rho\left(w_2^{(r)}\theta_3^{(r)}-w_3^{(r)}\theta_2^{(r)}\right)\right\}, \tag{22}$$
$$G_2=2h_1h_2\left\{\mu\theta_{3,3}^{(r)}\left(w_{1,3}^{(r)}-\theta_2^{(r)}\right)-Ew_{3,3}^{(r)}\theta_{1,3}^{(r)}+\lambda^{(r)}\rho\left(w_3^{(r)}\theta_1^{(r)}-w_1^{(r)}\theta_3^{(r)}\right)\right\}, \tag{23}$$
$$G_0=\Lambda AH. \tag{24}$$

The derived shape gradient function is utilized for obtaining the optimal shape by using the free-form optimization method for frame structures which will be explained in the next section.

Free-form optimization method for frame structures

The free-form optimization method for frame structures was developed by the authors for finding an optimal free-form shape of a frame structure (Shimoda, et al, 2013). It is a node-based shape optimization method based on the H^1 gradient method, which is a gradient method in a Hilbert space, and it can treat all nodes as design variables without shape parameterizations (Azegami and

Takeuchi, 2006, Shimoda, 2011). In this study, we applied this method to the natural vibration problem. In this method, the negative shape gradient function $-\boldsymbol{G}(=-G\boldsymbol{n})$ is applied as a distributed force to a fictious-elastic frame structure in the normal direction to the centroidal axis under a Robin boundary condition, i.e., an elastic support condition with a distributed spring constant $\alpha > 0$ as shown in Fig. 4. The stiffness matrix is used for the positive definite matrix required for a gradient method in a Hilbert space, and it also takes the role of a smoother to maintain the mesh regularity while reducing the objective functional. The shape variation $\boldsymbol{V} = (V_1, V_2, V_3)$ is determined in the fictious-elastic frame analysis, which is called velocity analysis, and the obtained $\boldsymbol{V}$ is used to update the shape. The governing equation of the velocity analysis for $\boldsymbol{V}$ is expressed as Eq. (25). The constraint conditions for velocity analysis are arbitrarily set by considering each individual shape design conditions.

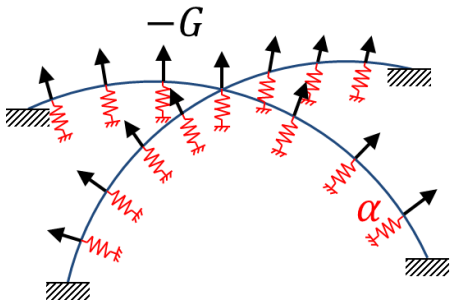

Figure 4. Schematic of the free-form optimization method for frame structures

$$a\left((\boldsymbol{V},\boldsymbol{\theta}),(\bar{\boldsymbol{w}},\bar{\boldsymbol{\theta}})\right)+\alpha\left\langle(\boldsymbol{V}\cdot\boldsymbol{n})\boldsymbol{n},(\bar{\boldsymbol{w}},\bar{\boldsymbol{\theta}})\right\rangle=-\left\langle G\boldsymbol{n},(\bar{\boldsymbol{w}},\bar{\boldsymbol{\theta}})\right\rangle,\ \forall(\bar{\boldsymbol{w}},\bar{\boldsymbol{\theta}})\in C_\Theta,\ (\boldsymbol{V},\boldsymbol{\theta})\in C_\Theta, \tag{25}$$

$$C_\Theta=\left\{(V_1,V_2,V_3,\theta_1,\theta_2,\theta_3)\in\left(H^1(S)\right)^6\middle|\text{satisfy Dirichlet condition for shape variation}\right\}. \tag{26}$$

In problems where convexity is assured, this gradient method reduces the Lagrange functional in the process of updating the frame shape using the design velocity field $\boldsymbol{V}$ determined by Eq. (25). The optimal free-form frame structure is obtained by iterating a process consisting of (1) eigenvalue analysis, (2) sensitivity analysis for calculating the shape gradient functions, (3) velocity analysis and (4) shape updating. The analyses in (1) and (3) are conducted using a general FEM code.

Calculated design examples

To verify the effectiveness and validity of the proposing optimization method for the natural vibration problems, two design problems are solved by using the developed system based on the method. Although the eigenvalue analyses were performed up to the 10 th mode, the result graphs shows only the modes related to the specified mode, and those modal orders at the initial shape are tracked through the plots.

Square frame model

The first design example is a square frame model having two cross members inside (size: 1000 ×1000). For all members, the cross sections are a square 20 on a side. Each of the circumference members and the cross members are meshed into 2 and 20 two-node elements, respectively, for a total of 48 elements. For this problem, the 1st eigenvalue is maximized and the design object is the cross members. The volume constraint was set as 1.05 times the initial value. Fig. 5(a) shows the initial shape and the boundary conditions for eigenvalue analysis and Fig. 5(b) shows the conditions

for velocity analysis. The numbers with a triangle in the figures express the single point constraint (SPC), and 1, 2, 3 express the X_1, X_2, X_3 translational degrees of freedom, respectively. Fig. 6(a) shows the initial 1st modal shape and Fig. 6(b) shows the obtained optimal shape, in which the cross members became smooth arches. The iteration convergence histories of the eigenvalue and the volume are shown in Fig. 6(c), where the values were normalized to those of the initial shape. Without switching to the higher modes, the eigenvalue was maximized at 1.26 times the value of the initial while satisfying the volume constraint.

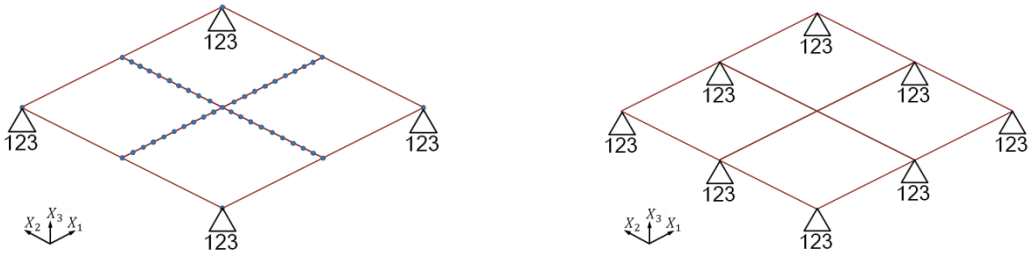

(a)Initial shape and B.C. for eigenvalue analysis (b) B.C. for velocity analysis

Figure 5. Initial shape and boundary conditions of square frame model

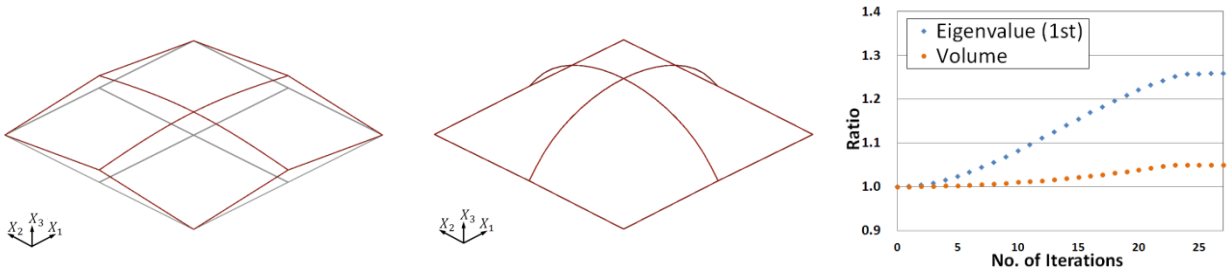

(a) 1st natural mode (b) Obtained shape (c) Convergence histories

Figure 6. Calculated results of square frame model

Portal frame model

The second design problem is concerned with a portal frame model (size: 3000 × 2800 × 600) as shown in Fig. 7(a). The cross sections are a square 10 on a side for the members that compose the sine-curved top lattice and a square 20 on a side for the side support members, respectively. All the members were meshed with two-node elements at the intersections of square grids, for a total of 398 elements. For this problem, the 2nd eigenvalue was maximized and the volume constraint was set as 1.01 times the initial value. Fig.7(a) shows the initial shape and the boundary conditions for eigenvalue analysis and Fig. 7(b) shows the conditions for velocity analysis. Fig. 8(a) shows the initial 2nd modal shape and Fig. 8(b) shows the obtained optimal shape, in which two beads were created along with the free edges and the side support members became slightly recurved. The iteration convergence histories of the eigenvalue and the volume are shown in Fig. 8(c), where the values were normalized to those of the initial shape. Without switching to the lower or higher modes, the eigenvalue was maximized at 6.40 times the value of the initial while satisfying the volume constraint.

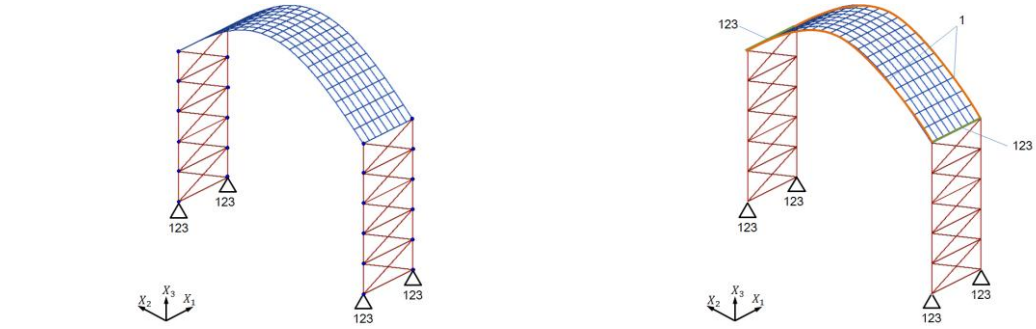

(a)Initial shape and B.C. for eigenvalue analysis (b) B.C. for velocity analysis

Figure 7. Initial shape and boundary conditions of portal frame model

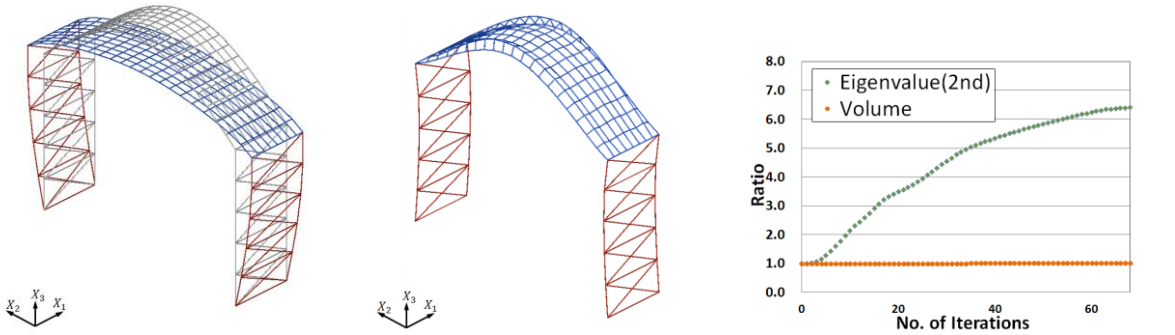

(a) 2nd natural mode (b) Obtained shape (c) Convergence histories

Figure 8. Calculated results of portal frame model

Conclusions

The free-form optimization method for frame structures was applied to the natural vibration problems that aim to maximize a specified eigenvalue. It is a node-based method that does not require any shape parameterization and it can efficiently find the smooth optimal shape for large scale problems under arbitrary shape design conditions. With the developed optimization system based on the proposing method, two design problems were solved and the validity and the effectiveness were confirmed.

References

Azegami, H. and Takeuchi, K.(2006), A smoothing method for shape optimization: Traction method using the Robin condition. *International Journal of Computational Methods*, 3, 21–33

Ohsaki, M. and Fujita, S. (2011), Multiobjective shape optimization of latticed shells for elastic stiffness and uniform member lengths, *Proceedings of International Symposium on Algorithmic Design for Architecture and Urban Design 2011, Tokyo*.

Choi, K. K. and Kim, N. H.(2005), Structural Sensitivity Analysis and Optimization, 1, *Springer, New York*

Hashemian, AH., Kargarnovin, MH. and Jam, JE. (2011), Optimization of geometric parameters of latticed structures using genetic algorithm, *Aircraft Engineering and Aerospace Technology*, 83, 59–68.

Kaveh, A. and Bakhshpoori, T. (2013), OPTIMUM DESIGN OF SPACE TRUSSES USING CUCKOO SEARCH ALGORITHM WITH LÉVY FLIGHTS, Transactions of Civil Engineering, Vol. 37, No. C1, pp 1-15

Shimoda, M.(2011), Free-form optimization method for designing automotive shell structures. *SAE, International Journal of Passenger Cars- Electronic and Electrical Systems*, 4, 42–54,

Shimoda, M., LIU, Y., and Morimoto, T. (2013*), Free-form Optimization Method for Frame Structures, *Structural and Multidisciplinary Optimization*, *submitted in 2013

Wang, D., Zhang, W. H., and Jiang, J. S. (2004), Truss Optimization on Shape and Sizing with Frequency Constraints, *AIAA Journal*, Vol. 42, No. 3, pp. 622-630.